Experimental investigation on interply friction properties of thermoset prepreg systems

Pasco, C., Khan, M., Gupta, J. & Kendall, K.

DOI 10.1177/0021998318781706
ISSN 0021-9983
ESSN 1530-793X

Publisher: Sage

Experimental Investigation on the Interply Friction Properties of Thermoset Prepreg Systems

Corentin Pasco*[1], Muhammad Khan[2], Jaipal Gupta[1], Kenneth Kendall[1],

[1] Automotive Composites Research Centre, WMG, The University of Warwick,

[2] Faculty of Engineering, Environment and Computing, Coventry University

*corresponding author email: c.pasco@warwick.ac.uk

Postal Address: WMG, The University of Warwick, International Manufacturing Centre, Gibbet Hill Road, Coventry CV4 7AL, United Kingdom

Abstract:

A comprehensive experimental characterisation of interply friction of thermoset prepregs with different reinforcement architecture (woven and unidirectional) consisting of the same rapid-cure resin system has been done at different processing parameters representative to those in high-volume processes such as press forming and double diaphragm forming. It has been reported that the two reinforcement forms exhibit significantly different frictional behaviour. The unidirectional material obeys a hydrodynamic lubrication mode. For the woven material, a rate-dependent friction behaviour was found at low normal pressure. At higher normal pressure however, the woven material exhibited a friction behaviour similar to that of a dry reinforcement and significant tows displacement was observed. Post-characterisation analysis of test-specimens showed significant resin migration towards the outer edges of the plies, leaving a relatively resin-starved contact interface. Current findings highlight a need to further investigate the influence of tensions as well as the impregnation level of plies on the friction properties.

Keywords: A. Prepreg, A. Thermosetting resin, E. Preforming, Interply friction,

1. Introduction

The increasing demand for fuel efficient vehicles has led to an increasing use of thermoset prepreg material due to their high specific strength and stiffness. This has consequently created a need for more efficient, less labour and capital-intensive manufacturing processes, as opposed to the more traditional autoclave method. Latest development in resin technology has made it possible to compression mould thermoset prepreg, offering short cycle times while retaining the exceptional mechanical performance of autoclaved prepreg [1-3]. Similar to traditional manufacturing methods, one of the first steps of prepreg compression moulding (PCM) is the preforming of an initial flat blank of material into its final 3D shape. Preforming of thermoset material can be automated and is typically done using press-forming [4], or double diaphragm forming [5, 6], prior to or as part of the curing stage (for double diaphragm forming) . Both these methods involve preheating a thermoset prepreg blank in order to lower the resin viscosity and to ease the deformation. Temperature must be carefully controlled as initiation of resin cure would increase the stiffness of the prepreg and prevent the material from deforming. The preheated blank is then transferred into a press for preforming and consolidation and curing (for double diaphragm forming). Irrespective of the preforming method, processing parameters i.e. temperature and forming speed have a significant influence on the quality of thermoset prepreg preforms. Preforming is a critical stage as it influences the structural property of the final part. The initial flat blank of prepreg material must deform in a predictable and repeatable way so that defects such as wrinkles, folds, fibre splitting and excessive fibre misalignments can be avoided. To date, a lot of effort has been carried out towards the numerical modelling of the preforming process. Preforming analysis can generate useful information for predicting manufacturing defects, assist in the forming tool design and create input for subsequent stress analysis, resulting in global optimisation of the product and process development. Preforming of multi-layered thermoset prepregs requires deforming the different plies to a desirable shape. This occurs through different deformation mechanisms such as intraply shear (shear within an individual ply), interply shear (or interply friction at the interface between neighbouring plies) and out-of-plane bending [7-9]. The accuracy of preforming simulation relies on the accurate description and characterisation of all these deformation mechanisms. In the present work,

experimental study on the interply shear of thermoset prepregs is carried out under similar conditions to those in press-forming and double diaphragm forming while preforming a multi-layer pre-stacked prepreg having plies with different relative orientation of fibre. The characterisation results are presented using the test conditions of relative slip velocity that are significantly higher than the previous investigations. While the friction behaviour at the interface ply/tool [10, 11], ply/diaphragm and diaphragm/tool [12] has been reported to influence the forming behaviour, it will not be considered in the present study.

2. Review of previous work

When preforming multi-layered prepregs, relative sliding of the plies might occur due to the presence of curved geometries. However, if sliding is prevented, compressive forces might build-up within the plies on the inside of a curve, leading to out-of-plane buckling. Previous studies [13-16] showed that processing parameters (i.e. temperature, forming rate and normal pressure) as well as material parameters (i.e. fibre lay-up and resin properties) significantly influence the interply friction coefficient. This results in cumbersome experimental work when one needs to perform a complete experimental characterisation. There exists two main friction models: Coulomb and hydrodynamic friction [14, 17]. Coulomb friction occurs between dry surfaces and is proportional to the normal pressure and independent of the sliding velocity while hydrodynamic friction occurs between two surfaces completely separated by a thin layer of fluid, and is as such generally shear rate dependent. Although there are standards to determine the coefficient of friction of plastic film and sheet, such as the ASTM D1894 [18], yet these do not take into account the influence of the fibrous reinforcement (i.e. architecture and orientation) and the resin. In addition, the ASTM D1894 only considers Coulomb friction. Therefore, most research on friction of composite material uses non-standard custom built rig, based on the pull-through or pull-out method [19]. A schematic of the pull-out method is shown in Figure *1*. This method was first developed by Murtagh et al [14] while testing the friction occurring between tooling and adjacent plies. A central specimen is drawn out from between two pressure plates, leaving a gap that introduces normal pressure inhomogeneity.

The pull-through method is shown in Figure *2*, and was developed by Wilks [20]. It consists of two fixed platens, and a moving platen, which clamps the specimen and is connected to a load cell. In that case, the specimen is pulled through the platens and the normal pressure stays constant.

Recently, an alternative approach of measuring the friction behaviour of composite material was presented, using a commercial rheometer [21]. Although this method allows the production of accurate data at a fast rate, however the pressure and rate achieved with this method are much lower than those typically obtained during preforming. Irrespective of the material and test method, load-displacement curves typically exhibit an initial peak followed by a steady state, corresponding to the static and dynamic friction, respectively [13, 19, 22, 23]. An exception has been observed for low displacement rate, where the static friction becomes indistinguishable. The static friction force is the force required to initiate slipping between adjacent plies while the dynamic friction is the force required to maintain sliding. In the absence of a standard test method, a benchmark study was conducted by seven institutions in order to compare friction test results using various test set-ups [24]. The different research groups determined the coefficient of friction between a metal surface and Twintex®PP (a thermoplastic composite of commingled glass fibre and polypropylene filaments) using the same test conditions at room temperature (dry friction) and elevated temperature (wet friction). For the dry friction coefficient, a difference of up to 32% between the participants was reported. In addition, in the case of dry friction tests, only the dynamic friction was stated as the static friction could not be determined by every research group. Regarding the wet friction, a relatively better agreement was found for the static friction than for the dynamic friction, which is thought to be due to boundary conditions and uneven pressure. These differences stress the need for a standard test method. In addition, while this benchmark study mostly applies for ply/tool, a similar study would be required for the friction behaviour of thermoset material at the ply/ply interface.

To date, a great majority of studies on friction behaviour of prepreg material have concerned thermoplastic composites [14, 15, 17, 20, 22, 25]. Thus, interply friction of thermoplastic composites is relatively well understood, and is generally considered as hydrodynamic [26].

Interply slippage is assumed to occur in a resin-rich layer between the plies, also described as a Couette flow, i.e. a viscous flow between two parallel plates [27]. This phenomenon was also demonstrated by Murtagh et al. [25] while investigating the interply slip mechanism of unidirectional thermoplastic material that occurs during press-forming. In the same study, they also observed a dependence of the reinforcement type (unidirectional and woven) on the frictional behaviour. From ply pull-out experiments, it was shown that the fabric material showed an initial stretching of the ply due to the crimp, followed by a shear rate dependent stationary friction (i.e. dynamic friction), while unidirectional materials show no initial fibre stretching. Such influence of the reinforcement architecture on the frictional behaviour had previously been observed by Ajayi [28], while studying the effect of woven fabric structure on frictional properties. He found that an increase in the yarn sett (i.e. the number of yarns per unit length) resulted in an increase in frictional resistance. In addition, it was found that friction coefficients depend on temperature and sliding velocity at elevated temperature only, supporting the assumption of a hydrodynamic lubrication mode. Also, it was observed that increasing normal pressure resulted in lower friction coefficient [14, 29]. The dependence of the friction coefficient on temperature (i.e. matrix viscosity), normal pressure and velocity led Chow [30] to make use of a Stribeck curve to interpret his experimental data. A Stribeck curve is a plot of the coefficient of friction as a function of the Hersey number expressed as:

$$H = \frac{\eta v}{p} \tag{1}$$

where η is the viscosity of the lubricating fluid, v is the velocity and p is the normal force acting on the contact surface. Figure *3* illustrates a typical Stribeck curve and shows the three different lubrication regimes, i.e. boundary lubrication (the film fluid is negligible, resulting in friction similar to Coulomb friction), elasto-hydrodynamic lubrication (mixed-mode lubrication) and hydrodynamic or full-film lubrication (surfaces are completely separated by a fluid film). The Stribeck curve provides a qualitative explanation of the mechanism governing friction for a range of processing parameters (i.e. normal pressure, slip velocity and resin viscosity through temperature of the plies) by plotting the friction coefficient as a function of the Hersey number.

The Stribeck theory has been used by several researchers to analyse and model the friction behaviour of composite materials [31-33].

Unlike thermoplastic material, literature on friction properties of thermoset material is relatively scarce. In addition, the vast majority of published papers apply to processes destined for the aerospace industry [13, 23, 29]. As such, the range of parameters used is not applicable to high volume manufacturing processes (e.g., extremely slow slip velocities were used together with normal pressure obtained in autoclave). Martin et al [23], studied the frictional properties of three aerospace graded woven thermoset prepreg at the ply/ply interface, in order to understand the influence of the interply slip on core crush of autoclaved honeycomb sandwich structure. Using a pull-through test at temperature and pressure representative of a typical autoclave cure cycle (i.e. pressure ranging from 200 kPa to 500 kPa) it was found that the frictional forces of the prepreg helps prevent core crush by limiting slip, no mention of the slip velocity was made. It was also found that friction coefficient depends on the prepreg system as well as the temperature. Prepreg with higher resin viscosity together with a high amount of resin at the surface showed lower frictional resistance. As the temperature increases, the resistance to slip decreases until a minimum, which suggests that interactions between the surfaces occur, most likely by intermingling of the fibres from the plies in contact. This phenomenon was also notice by Ersoy et al [29]. They investigated the frictional properties of a unidirectional carbon /epoxy aerospace graded material in order to understand the effect leading to the formation of residual stresses within parts manufactured by autoclave process. A pull-out test and a rate between 0.01 and 0.10 mm/min, a normal pressure of 700 kPa and a varying temperature were used, in order to simulate the autoclave curing cycle. At the ply/ply interface, they found that the lay-up has an influence in the frictional properties, and particularly that plies oriented at 90° in a $[0/90]_s$ lay-up prevented transfer of stresses between the 0° plies. While studying the interply friction of thermoset unidirectional materials, Larberg et al [13], observed a friction behaviour more complex than purely hydrodynamic, as opposed to thermoplastic material. One of the materials tested exhibited a rate independent behaviour, indicating boundary lubrication. It was also found that the friction coefficient decreased with normal pressure until reaching a steady value, typical of a boundary lubrication mode. Friction load versus displacement curves

obtained during a friction test were reported over a maximum cross-head displacement of 2.5mm. However, in some cases, relative slip between plies when preforming a part can reach more than 70mm [34]. It is important to study the evolution of the friction properties over the maximum possible range of interply slip, particularly in the case of woven material, where interactions and movements between the tows in contact are expected due to the architecture of the material.

Thermoset prepreg materials are well suited for the manufacture of complex automotive components. However, in the context of high-volume manufacturing, their implementation is facing many challenges. One of the main limitations is the lack of research work and experimental data on the deformation behaviour on these materials, particularly under conditions similar to those found in high-volume processes. Recent contributions in the study of frictional behaviour of thermoset are limited to unidirectional reinforcements [13]. In this paper, the influence of the sliding velocity and the normal pressure on the frictional properties of two thermoset prepreg reinforcements will be studied. The same resin system is used in both materials (i.e. a fast cure epoxy resin), but the reinforcements have different architectures. One is 2x2 twill weave and the other a unidirectional carbon fibre material. This will allow for a direct comparison of the effect of the reinforcement architecture on the interply friction behaviour. The test conditions of relative slip velocity used in this investigation are significantly higher than those commonly used in previous studies. This warrants to implement the characterisation data on friction mechanisms for higher volume applications. Material behaviour and deformation mechanisms occurring during the test and implications on test-rig design will be discussed, particularly when testing woven prepreg material. Further, guidelines and recommendations on the test-rig design and characterisation procedure are proposed as a consequence of this investigation.

3. Experimental

3.1. Material investigated

The materials used in this study are a unidirectional and a 2x2 twill weave reinforcement architectures for thermoset prepreg systems. The unidirectional material has a fibre areal weight

of 250 g/m², a 15k tow-size and a resin content of 30% by weight while the woven material has a fibre areal weight of 400 g/m², a 12k tow-size and a resin content of 40% by weight. The prepreg materials investigated are based on the same epoxy rapid cure thermoset resin, which allows for a direct comparison of the reinforcement effect on the interply friction properties. Indeed, it has been shown that friction coefficient depends on resin viscosity which itself depends on the chemistry. Consequently, at a given temperature, the viscosity of different prepregs material can vary [13]. Both materials have been specifically designed for compression moulding and are suitable for high volume applications, with a typical curing time of 5 minutes at 140°C. Curing time can be adjusted depending on the moulding temperature. The material supplier is Mitsubishi Chemical Carbon Fiber and Composites. Figure *4* shows images of the prepreg materials.

Due to the high reactivity of the resin, differential scanning calorimetry (DSC) analysis was carried out in order to investigate the relationship between the onset of cure and time. This allows to determine, for a given temperature, the maximum allowable heating time before the initiation of cure. The results are then used as an upper bound for the friction test soaking time. Past the onset of cure, the resin viscosity starts rising and prevent material deformation and ply slippage during preforming.

3.2. Test rig

The interply friction was measured using a specifically designed test rig. The apparatus is shown in Figure *5*, and consists of two parallel, stationary outer platens and one moving centre platen. Due to the high thermal masses and the packaging size of the rig, it was found that using a thermal chamber alone, a soaking time of an hour was required in order to reach a temperature of 80°C at the interface between the plies. Considering the high reactivity of the material and for practical reasons, this was not suitable. Therefore, all three metallic platens have been equipped with cartridge heaters connected to a two zone temperature controller, producing a total of 4,400 watts and allowing to heat the rig at a temperature of 80°C in under a minute. The centre plate is fitted to a 500N load cell, attached to the cross-head of Instron 5800R. The cross-head moves at a constant set velocity and its displacement is recorded every

0.1 seconds. Normal pressure upon the material is applied by means of four linear compression springs that can be tightened or loosened using nuts. The pressure is adjusted to a set value by controlling the linear displacement of the springs together with the torque applied to the adjusting nuts. Three prepreg specimens were used for each test: one sample was wrapped around the moving platen and two samples were mounted and clamped on the outer platen. The resultant testing contact surface area was 8,192mm^2 and remained constant throughout the duration of the test. When testing the unidirectional material, specimens on the outer platens can be oriented at 0° and 90° to the pulling direction, making it possible to test the friction properties between different relative fibre orientations (i.e. either 0°/90° interface or 0°/0°). For the unidirectional material, the specimen on the centre platen can only be mounted with its fibre parallel to the pulling direction. Other orientations would lead to tearing the specimen apart due to the lack of integrity in the transverse direction.

To start a test, the prepreg material specimens were first placed and clamped on the platens. The normal force was then adjusted and the rig was heated up. Once the temperature reached 80°C, a soaking time of 2 minutes was used in order to ensure a homogenous temperature distribution at the testing surfaces. Temperature at the ply/ply interface was controlled using a thermocouple. Then, the tangential load and the displacement were measured. At least three samples were tested for each test condition.

3.3. Test variables

In the present study, all specimens were tested at a temperature of 80°C, which is a typical preforming temperature [35]. A higher temperature would lead to the initiation of the curing process while a lower temperature would result in a high resin viscosity. Both situations would hinder shearing of the resin, ultimately preventing the ability of the material to deform during preforming. The viscosity-temperature curve for the resin investigated is shown in Figure *6*. It can be seen that from room temperature to 80°C, the viscosity drops drastically by approximately three orders of magnitude. While an increase of the temperature would further decrease the viscosity, the time-temperature dependence of the viscosity in Figure *7* shows that at a higher temperature, i.e. 110°C, the resin reactivity significantly increases and could become

a limiting factor when preforming. Interply friction tests were carried out using three different velocities: 1, 5 and 10 mm/s and four different normal pressures, 25, 50, 75 and 100kPa. The velocities and pressure used conform to the preforming conditions suitable for press-forming and double diaphragm forming. In addition it has been shown that the resin behaves as a Newtonian fluid, i.e. the viscosity is independent of the shear velocity whilst the shear stresses increase linearly with increasing shear velocity (Figure *8*).

4. Results and discussion

The results of the friction tests are presented and explained in the next sections. The effect of normal pressure and sliding velocity on the frictional behaviour of the two materials are discussed and compared. For each unique set of test variables, the experimental results were averaged over three samples. The error bars represent one standard deviation on either side of the averaged results. For clarity's sake, all data presented on each figure have been plotted on the same scale.

4.1. Unidirectional material

Figure *9* shows load versus displacement graphs, which illustrate the influence of the normal pressure on the frictional behaviour of unidirectional material, tested at different sliding rate. For all tests, the fibre orientation at the contact interface was 0°/90°. It can be observed that irrespective of the normal pressure and the sliding velocity, the results exhibit the same general trend. First, the frictional force increases rapidly up to a maximum peak, corresponding to the static friction or the force required to initiate sliding between surfaces. Secondly, the force decreases and eventually reaches a steady state, corresponding to the dynamic friction. For each test rate, both the static and the dynamic friction forces increase with increasing normal pressure (Figure *9*). As the normal pressure increases, higher tangential forces are required to pull the adjacent surfaces apart. It can also be observed that the spread of the static friction seems to be pressure and rate dependent. As the normal pressure increases, the static friction peak spreads over a greater displacement (Figure *9*). This is particularly noticeable for medium to high sliding velocity, i.e. 5 and 10mm.s-1 where the spread ranges from approximately 10mm

displacement at 25kPa to 30mm displacement at 100kPa. At a test rate of 1mm.s-1, this phenomenon is less obvious. In addition, the amplitude of the static friction with respect to the dynamic plateau decreases with increasing pressure. Indeed, for a given test speed, the ratio between the static friction load and the dynamic friction load is greater at 25kPa than 100kPa. Therefore, the effect of normal pressure on the frictional behaviour is different on the static friction and the dynamic friction. This is because both types of friction arise from different mechanisms. Static friction has been associated with adhesion mechanisms and chemical interactions between opposing surfaces [36]. At an atomic-scale, static friction is non-existent between two clean crystalline surfaces under ultra-high vacuum. However, in the macroscopic world, two objects sliding against each other always exhibit static friction. Gang et al. [37], proposed an explanation whereby there exists "third bodies" in the form of adsorbed molecules, that act to lock the two contacting surfaces together that have been exposed to air. It was also shown that static friction is an exponential function of time. The longer the surfaces are in contact, the higher the static friction coefficient [38]. One possible explanation is that when surfaces stay stationary, the lubricant (i.e. the resin in this case) is drawn into the cavities, leading to higher meniscus force and consequently higher static friction. Similarly, an increase in normal pressure will force the resin into these cavities, increasing wetting between mating surfaces and therefore increasing static friction. The time-dependency of the static friction behaviour was not investigated in this study. However, the effect of time was controlled using a constant soaking time between each test. Dynamic friction on the other hand is related to energy losses created at the interface during sliding [39].

It is interesting to note that all curves, except those tested at 10mm.s^{-1} appear jagged rather than smooth, past the static peak. This phenomenon is a characteristic of stick-slip frictional behaviour and has also been observed with woven fabrics [28, 40]. Stick-slip can be explained by the successive formation and rupturing of new interfaces between two surfaces, leading to the occurrence of static friction peaks and sliding. This phenomenon is time-dependent and seems to disappear at higher sliding speed as there is not sufficient time for the formation of adhesion contacts to occur resulting in a smooth sliding [41].

Figure *10* shows the influence of the sliding rate on the frictional behaviour of unidirectional material, tested at different normal pressure. It can be observed that for a given normal pressure, the static and dynamic friction behaviour is velocity dependent. For each normal pressure, the static and dynamic friction forces increase as the sliding velocity increases. This suggests the presence of lubricated, viscous sliding rather than boundary lubrication effects.

This can be directly related to the presence of the viscous, shear rate dependent resin. However, it is interesting to see that the evolution of the dynamic friction with increasing slipping rate is less obvious for the specimens tested at 25kPa than that observed for the specimens tested at higher normal pressures. In other words, the effect of rate dependence tends to become smaller at 25kPa. The ratio between the dynamic loads measured at $10mm.s^{-1}$ and $1mm.s^{-1}$ is approximately 1.4 at a normal pressure of 25kPa while it varies between 2.26 and 2.5 for other normal pressures suggesting that the friction modes may be different. The use of a low normal pressure of 25kPa may create higher surface roughness at the interface between two plies, resulting in larger dry contact areas. On the other hand, higher normal pressures may force the resin to migrate through the reinforcement towards the contact interface forming a resin film and providing a lubricated, rate dependent mode of friction. In contrast, the relative evolution of the static friction as a function of the sliding rate is similar for each normal pressure. For all normal pressure considered, the ratio of the static load measured at $10mm.s^{-1}$ to the load measured at $1mm.s^{-1}$ varies between 2.25 to 2.4.

The evolution of the static and dynamic friction coefficients as a function of the different parameters investigated is shown in Figure *11*. The friction coefficients were calculated such that:

$$\mu = \frac{F}{2 \times a \times N} \tag{2}$$

Where, *F* is the tangential load read by the load cell, *a* is the surface area of the two side plates and *N* is the normal pressure. The tangential load used for the calculation of the static friction coefficients corresponds to the highest load obtained from the load versus displacement traces. For the determination of the dynamic friction coefficients, the load used for the calculation

corresponds to the average of the loads ranging between the intersection of the tangent of the peak with the plateau to the end of the test. It can be seen that both the static and the dynamic friction coefficients increase with increasing sliding velocity and decrease with increasing normal pressure. The friction coefficient-velocity relationship is quasi-linear, which suggests that friction is characterised by shearing of the Newtonian epoxy matrix present at the interface (i.e. by definition, shear stresses increase linearly with increasing shear rate). In contrast, in all cases but the dynamic friction tested at $10mm.s^{-1}$, friction coefficients show an asymptotic relationship with the normal pressure. Both static and dynamic friction coefficients decrease with increasing normal pressure before reaching a minimum value and plateau.

One explanation is that for low normal pressures, interlocking and nesting between opposing fibres having initially circular cross-section is likely to occur, resulting in a rough surface contact. However, for higher normal pressures, opposing fibres as well as any asperities at the interface will be flatten out, thus resulting in a reduction of the roughness and consequently, the friction coefficients. This was also observed in [13] and [42]. Upon increasing normal pressure, no further compaction seems possible as the coefficient values plateau. This behaviour corresponds to the region characteristic of a hydrodynamic regime (see Stribeck curve Figure *3*), where the friction coefficients decrease with increasing normal pressure and increase with increasing sliding speed. Dark-field micrographs of the cross-section of specimens along the sliding direction, taken after a test are shown in Figure *12* and correspond to specimens tested with a normal pressure of 25 and 100 kPa on the left and the right side, respectively.

The dividing area between the specimen mount and the sample correspond to the black lines at either side of the specimen. For both tests with a normal pressure of 25kPa and 100kPa, there does not seem to be any voids within the plies (characterised by dark and round-shaped spots). This suggests that the plies are fully impregnated and that therefore, some degree of lubrication was present during the tests. The interface is perfectly discernible and no disturbances and interactions between the fibres are visible. The distance reported on the micrographs show that a normal pressure of 100 kPa leads to a greater degree of compaction compared to a lower normal pressure. The global laminate thickness after performing the test with a normal pressure

of 100kPa is 449µm on average, while it was 482µm on average for the test with a normal pressure of 25kPa. Figure *13* summarises the friction coefficient data for both the static and dynamic states for the unidirectional material.

4.2. Woven material

The woven material was tested under the same conditions as those used for the UD material. All tests were performed with the warp direction parallel to the sliding direction. Indeed it was seen that pulling the material along the weft direction increase the risk of damaging the fabric [43]. Figure *14* shows the effect of normal pressure on the tangential load for different sliding velocity.

Similar to the UD material, for a given sliding speed, the tangential load increases with increasing normal pressure. However, the evolution of the tangential load exhibits a different trend depending on the test condition. At a sliding velocity of $1mm.s^{-1}$, it can be seen that initially, the load increases rapidly up to a peak of local maximum. Past the initial peak, the load decreases before increasing again to reach a plateau at a displacement of approximately 20mm. The load decrease is particularly more distinct for higher normal pressures, i.e. 75kPa and 100kPa. This is most likely due to initial movement and displacement of the specimens relative to the platen on which they are supported, as the test begins. This is also accompanied by uncrimping of the tows. Until the material is fully taut, it is difficult to interpret the data as the tangential loads result from a combination of different mechanisms. As a consequence, the transition between static to dynamic friction is not obvious, and therefore, only the dynamic friction will be reported in the next sections. At a sliding velocity of 5 and $10mm.s^{-1}$, the general shape of the load-displacement curves is more similar to that of the UD material at similar test conditions in that there is no significant load decrease before the occurrence of the dynamic regime, i.e. after approximately 20mm extension.

Figure *15* shows the influence of the sliding rate on the load-displacement curves at different normal pressures. It can be seen that the effect of the sliding velocity mostly affects the evolution of the tangential force over the first 20mm of displacement, for the tests performed

with a high normal pressure. However, past this point, the effect of the sliding velocity on the dynamic friction forces of the woven material is relatively small, unlike the UD material, and decrease with increasing normal pressure. Because both prepreg reinforcements have the same resin system, i.e. a fast cure epoxy resin, this different behaviour suggests that the interply slip process of the two materials involve different mechanisms and is affected by the reinforcement architecture. While the general trend of the load-displacement curves of the UD material is similar irrespective of the test conditions, it largely differs on the normal pressure for the woven material.

This different behaviour is directly related to the structure of the woven material. Evaluation of the specimen after tests revealed that the interply friction of woven prepreg at high normal pressure is accompanied with significant localised movement of transverse tows. Figure *16* shows two specimens after a friction test performed with a sliding rate of 1mm.s-1 and a normal pressure of 25kPa (a) and 100kPa (b). The specimen tested with a normal pressure of 25kPa shows no sign of tows displacement. In contrast, the specimen tested with a normal pressure of 100kPa shows a transverse tow that has been pulled-out along the sliding direction.

Because the transverse tows are free at their both ends, they have a higher propensity to move due to frictional forces, as compared to the longitudinal fibres that are restricted by the clamping. In this case, displacement of transverse tows is solely due to frictional forces exerted by the mating surface. During preforming of woven reinforcements, this deformation mode can occur and typically results to in-plane waviness. In practise, such issues can be overcome using techniques that increase axial tensions in the tows and limit in-plane waviness and wrinkling. These typically include blank holders and grippers for matched die forming and vacuum pressure for double diaphragm forming. The development of tensile and compressive forces within the tows of a fabric reinforcement will strongly influence the frictional behaviour of woven material. Indeed, increasing axial tension in the warp and weft tows will reduce crimp and consequently flatten the surface of the ply, while a relatively loose tow will be more likely to move, similar to that seen in Figure *16*.

This observation raises important, new implications for the characterisation of the frictional properties of woven materials, particularly when applied for preforming processes involving high normal pressure such as double diaphragm forming. In order to get accurate and representative data, an understating of all stresses within the fabric is required.

Similar to the UD material, friction coefficients can be calculated from the tangential loads. Figure *17* summarises the evolution of the dynamic friction coefficients as a function of sliding velocity and normal pressure. Firstly, it can be seen that the evolution of the dynamic friction coefficients with normal pressure depends on the sliding velocity. While the results from the tests performed at 1 and 10mm.s^{-1} exhibit a similar and expected trend, i.e. the dynamic friction coefficients decrease with increasing normal pressure similar to the UD material, the test performed at 5mm.s^{-1} do not show such a clear trend. In addition, the effect of the sliding velocity on the dynamic friction coefficients varies depending on the normal pressure. For lower normal pressure of 25 and 50kPa, the dynamic friction coefficient remains constant with a sliding velocity of 1 and 5mm.s-^{1}, while a further increase of the sliding velocity leads to an increase of the dynamic friction coefficient. For a normal pressure of 75kPa, the frictional behaviour seems rate dependent as the friction coefficient increases with increasing testing rate.

For a normal pressure of 100 kPa, it can be seen that the evolution of the sliding velocity on the dynamic friction coefficients is almost negligible. Indeed, the dynamic friction coefficients are similar at 1 and 10mm.s^{-1}. This suggests that for normal pressure similar to those obtained during double diaphragm forming, i.e. 1 bar, the frictional properties of woven material are rate independent, and that the material behave as a dry reinforcement, unlike the UD material. This is rather unexpected as the woven material has a higher resin content by weight than the UD material. One possible explanation can be related to the manufacturing process of out-of-autoclave prepreg material and their different degree of impregnation. These reinforcements are only partially impregnated and exhibit resin rich areas on both outer surfaces of the ply, while the centre remains dry and porous (Figure *18*). The porous medium is sometimes referred to as engineered vacuum channels (EVaCs) and facilitates migration of trapped air and gas towards

the boundaries of the ply in the early moulding stage. During compaction, the dry areas are then progressively infiltrated with resin to produce a void-free structure.

High normal pressure exerted during friction tests caused the resin on both surfaces to squeeze out of the contact interface between the two plies.**Error! Reference source not found.** Figure 19 shows the surface of a specimen after a friction test performed with a normal pressure of 100kPa. On the top half of the picture, a relatively thick and shiny layer of resin can be observed and corresponds to an area of the ply that has not been in contact with another ply. In contrast, the bottom half of the picture show dry fibres and corresponds to an area of the specimen that was in contact with the mating surface during the friction test. Consequently, with a normal pressure of 100kPa, the contact interface was not fully lubricated. When testing frictional properties of a dry carbon twill weave reinforcement at 5mm.s-1s Allaoui et al. [44], found a dynamic friction coefficient of approximately 0.3, similar to the one obtained in this study at 100kPa. This confirms the assumption that the frictional properties of the woven prepreg at high normal pressure are similar to those of a dry fabric.

Scanning electron microscopy (SEM) micrographs of the cross-section of a specimen taken after a test performed with a normal pressure of 25kPa and 100kPa are shown in Figure 21. Specimens were imaged using a Sigma Zeiss FEG SEM under InLens imaging mode with a 20kV accelerating voltage. Samples were placed on an aluminium stub coated with adhesive carbon table and held vertically using mounting clips to image the cross-section of the specimen. Samples were sputter coated with a Pd/Au prior to imaging. The dashed white lines represent the interface between the two woven plies. For the specimen at 25kPa, the fibres can be seen within a thick layer of resin, particularly near the interface. Lack of compaction due to low normal pressure can be seen at the interface between the warp and weft of the ply located at the left-hand side of the micrograph. In contrast, the micrograph of the specimen tested at a normal pressure of 100kPa shows a relatively dry interface. Unlike the other specimen, the fibres at the interface can be seen individually and do not seem to be immersed within the resin. In addition, resin rich areas characterised by a shiny and milky appearance can be observed on

both outer surfaces of the specimen. The higher normal pressure has caused the resin to migrate from the contact interface towards the outside of the specimen, leaving a dry interface.

4.3. Stribeck analysis

Friction coefficients can be plotted as a function of the Hersey number which is a function of the normal pressure, viscosity and velocity. In that case the viscosity is of the bulk resin at 80°C. The curve generated can then be related to the Stribeck curve (see Figure *3*). For the UD material, the curve corresponds to the hydrodynamic (full-film) lubrication mode (Figure 21). For the woven material however, a more complex behaviour is seen. A linear fitting gives a poor R-squared value, and cannot be linked to any specific lubrication regime. Consequently, depending on the test parameters the frictional behaviour of the woven prepreg extends across different types of lubrication regime.

5. Conclusions and perspectives

The interply frictional behaviour of prepreg materials for two different types of reinforcement, i.e. a woven twill and a UD reinforced prepreg both using the same epoxy resin system was measured using a dedicated rig. The influence of the sliding velocity as well as the normal pressure, representative of those used for high-volume processing were investigated. It was shown that both reinforcements exhibit a very different behaviour. The UD material showed predictable results: (1) the friction coefficients increase with increasing sliding velocity due to the shear rate dependence of the resin at the contact interface and (2), the friction coefficients decrease with increasing normal pressure due to a reduction in global surface roughness at the interface. Stribeck curve analysis was used to predict the behaviour of the different materials. The UD material shows a hydrodynamic type of lubrication, i.e. the surfaces are kept apart by an unbroken film of lubrication.

In contrast, the woven material showed more complex results due to the nature of its architecture and the different mechanisms observed during the tests. Similar to the UD prepreg, friction coefficients seemed to decrease with increasing normal pressure. However, the influence of the sliding velocity was relatively different. While the material showed a slip rate

dependence at low normal pressure, it behaves differently at high normal pressure. The partial impregnation of the woven prepreg combined with a high normal pressure resulted in a frictional behaviour similar to that of a dry reinforcement. SEM micrographs of samples tested at 100kPa showed resin migration towards the outside of the specimen, leaving a contact interface resin-starved and causing the reinforcement to behave as a dry fabric. Unlike the UD material, the woven prepreg does not fit within any particular regime of lubrication of the Stribeck curve. This highlighted the complex behaviour of the material and suggested that, depending on the sliding velocity and normal pressure conditions, the frictional behaviour of the woven material exhibits a different lubrication regime. In addition, analysis of woven test specimens at the macro-scale level revealed significant transverse tows movement when tested at high normal pressure highlighting the influence of axial tension within the warp and weft.

The findings of this work provide useful perspectives for further work: (1) it was seen that the occurrence of excessive tension within warp and weft led to the displacement and in-plane waviness of individual tows. This parameter needs to be further investigated and is of significant importance for preforming processes such as matched die forming and double diaphragm forming where the development of tension within the reinforcement occurs. Current friction test methods do not make it possible to adust the tension in both warp and weft tows. (2) The partial impregnation of the woven material (i.e. the material is not uniformly impregnated across the whole thickness) combined with high normal pressure led to a migration of the resin towards the outer surfaces of the specimen. This behaviour is expected to be different for a fully impregnated material. Consequently, the influence of the degree of impregnation of the prepreg on its interply friction behaviour should be investigated. This parameter is particularly important for preforming processes such as double diaphragm forming where the laminate is typically preheated in between the diaphragm membranes under vacuum, thus modifying the impregnation level.

Acknowledgement

This work was jointly funded by EPSRC and Aston Martin Lagonda Limited.

References

1. Akiyama, K. *Development of PCM* technology*. in *SPE Automotive and Composites Divisions - 11th Annual Automotive Composites Conference and Exhibition, ACCE 2011*. 2011. Troy, Michigan, USA.
2. Malnati, P., *Prepreg compression molding makes its commercial debut.* High-Performance Composites, 2015(JUNE, 2015).
3. Pasco, C. and K. Kendall. *Characterisation of the thermoset prepreg compression moulding process*. in *SPE Automotive and Composites Divisions - 16th Annual Automotive Composites Conference and Exhibition, ACCE 2016*. 2016. Novi, Michigan, USA.
4. Khan, M.A., et al., *Processing of thermoset prepregs for high-volume applications and their numerical analysis using superimposed finite elements.* Composite Structures, 2015. **131**: p. 917-926.
5. Bersee, H.E.N., et al. *Diaphragm forming of thermoset composites*.
6. Bernsdorf, M. *Process & Resin Development for BMW M4 GTS hood program*. in *SPE Automotive and Composites Divisions - 16th Annual Automotive Composites Conference and Exhibition, ACCE 2016*. 2016. Novi, Michigan, USA.
7. Boisse, P., et al., *Composites forming*, in *Advances in Material Forming*. 2007, Springer. p. 61-79.
8. Long, A.C., *Composites Forming Technologies*. Woodhead Publishing Series in Textiles. 2014: Elsevier Science.
9. Gereke, T., et al., *Experimental and computational composite textile reinforcement forming: A review.* Composites Part A: Applied Science and Manufacturing, 2013. **46**: p. 1-10.
10. Kaushik, V. and J. Raghavan, *Experimental study of tool–part interaction during autoclave processing of thermoset polymer composite structures.* Composites Part A: Applied Science and Manufacturing, 2010. **41**(9): p. 1210-1218.
11. Potter, K.D., et al., *The generation of geometrical deformations due to tool/part interaction in the manufacture of composite components.* Composites Part A: Applied Science and Manufacturing, 2005. **36**(2): p. 301-308.
12. Monaghan, M.R. and P.J. Mallon, *Study of polymeric diaphragm behaviour in autoclave processing of thermoplastic composites.* Broadening horizons with advanced materials and processes, 1993: p. 283-299.
13. Larberg, Y.R. and M. Åkermo, *On the interply friction of different generations of carbon/epoxy prepreg systems.* Composites Part A: Applied Science and Manufacturing, 2011. **42**(9): p. 1067-1074.
14. Murtagh, A.M., J.J. Lennon, and P.J. Mallon, *Surface friction effects related to pressforming of continuous fibre thermoplastic composites.* Composites Manufacturing, 1995. **6**(3–4): p. 169-175.
15. Scherer, R. and K. Friedrich, *Inter-and intraply-slip flow processes during thermoforming of CF/PP-laminates.* Composites Manufacturing, 1991. **2**(2): p. 92-96.
16. Larberg, Y.R., M. Åkermo, and M. Norrby, *On the in-plane deformability of cross-plied unidirectional prepreg.* Journal of composite materials, 2012. **46**(8): p. 929-939.
17. Murtagh, A.M. and P.J. Mallon, *Chapter 5 Characterisation of shearing and frictional behaviour during sheet forming*, in *Composite Materials Series*, D. Bhattacharyya, Editor. 1997, Elsevier. p. 163-216.
18. *ASTM D1894-14, Standard Test Method for Static and Kinetic Coefficients of Friction of Plastic Film and Sheeting*. 2014, ASTM International: West Conshohocken, PA.

19. Harrison, P., et al., *Characterising and modelling tool-ply friction of viscous textile composites.* World Journal of Engineering, 2010. **7**(1): p. 5-22.
20. Wilks, C.E., *Processing technologies for woven glass/polypropylene composities.* 1999.
21. Lin, H., et al. *Investigation of tool-ply friction of viscous textile composites*. in *8th International Conference on Textile Composites, TexComp 2006*.
22. Morris, S.R. and C.T. Sun, *An investigation of interply slip behaviour in AS4/PEEK at forming temperatures.* Composites Manufacturing, 1994. **5**(4): p. 217-224.
23. Martin, C.J., J.C. Seferis, and M.A. Wilhelm, *Frictional resistance of thermoset prepregs and its influence on honeycomb composite processing.* Composites Part A: Applied Science and Manufacturing, 1996. **27**(10): p. 943-951.
24. Sachs, U., et al., *Characterization of the dynamic friction of woven fabrics: Experimental methods and benchmark results.* Composites Part A: Applied Science and Manufacturing, 2014. **67**: p. 289-298.
25. Murtagh, A.M. and P.J. Mallon. *Shear characterisation of unidirectional and fabric reinforced thermoplastic composites for pressforming applications*. in *10th ICCM Conference (Canada)*. 1995.
26. Vanclooster, K., S.V. Lomov, and I. Verpoest, *Simulation of multi-layered composites forming.* International Journal of Material Forming, 2010. **3**: p. 695-698.
27. Cattanach, J.B. and F.N. Cogswell, *Processing with Aromatic Polymer Composites*, in *Developments in Reinforced Plastics—5: Processing and Fabrication*, G. Pritchard, Editor. 1986, Springer Netherlands: Dordrecht. p. 1-38.
28. Ajayi, J.O., *Effects of Fabric Structure on Frictional Properties.* Textile Research Journal, 1992. **62**(2): p. 87-93.
29. Ersoy, N., et al., *An experimental method to study the frictional processes during composites manufacturing.* Composites Part A: Applied Science and Manufacturing, 2005. **36**(11): p. 1536-1544.
30. Chow, S., *Frictional interaction between blank holder and fabric in stamping of woven thermoplastic composites.* Department of Mechanical Engineering, 2002.
31. Aimene, Y., et al., *Hyperelastic approach for composite reinforcement forming simulations.* International Journal of Material Forming, 2008. **1**(1): p. 811-814.
32. Gorczyca, J.L., et al., *Modeling of friction and shear in thermostamping of composites-part I.* Journal of Composite Materials, 2004. **38**(21): p. 1911-1929.
33. Gorczyca-Cole, J.L., J.A. Sherwood, and J. Chen, *A friction model for thermostamping commingled glass–polypropylene woven fabrics.* Composites Part A: Applied Science and Manufacturing, 2007. **38**(2): p. 393-406.
34. Allaoui, S., C. Cellard, and G. Hivet, *Effect of inter-ply sliding on the quality of multilayer interlock dry fabric preforms.* Composites Part A: Applied Science and Manufacturing, 2015. **68**: p. 336-345.
35. Akiyama, K. *Development of preforming process in PCM (Prepreg Compression Molding) technology*. in *SPE Automotive and Composites Divisions - 12th Annual Automotive Composites Conference and Exhibition, ACCE 2012*. 2012.
36. Zhang, Q., et al., *Origin of static friction and its relationship to adhesion at the atomic scale.* Physical Review B, 2007. **75**(14): p. 144114.
37. He, G., M.H. Müser, and M.O. Robbins, *Adsorbed Layers and the Origin of Static Friction.* Science, 1999. **284**(5420): p. 1650.
38. Tu, C.-F. and T. Fort, *A study of fiber-capstan friction. 2. Stick–slip phenomena.* Tribology International, 2004. **37**(9): p. 711-719.
39. Braun, O.M. and A.G. Naumovets, *Nanotribology: Microscopic mechanisms of friction.* Surface Science Reports, 2006. **60**(6–7): p. 79-158.

40. Hosseini Ravandi, S.A., K. Toriumi, and Y. Matsumoto, *Spectral analysis of the stick-slip motion of dynamic friction in the fabric surface.* Textile research journal, 1994. **64**(4): p. 224-229.
41. Drummond, C., J. Israelachvili, and P. Richetti, *Friction between two weakly adhering boundary lubricated surfaces in water.* Physical Review E, 2003. **67**(6): p. 066110.
42. Kalebek, N.A. and O. Babaarslan, *Effect of weight and apllied force on the friction coefficient of the spunlace nonwoven fabrics.* Fibers and Polymers, 2010. **11**(2): p. 277-284.
43. Sachs, U., *Friction and bending in thermoplastic composites forming processes*. 2014: University of Twente.
44. Allaoui, S., et al., *Influence of the dry woven fabrics meso-structure on fabric/fabric contact behavior.* Journal of Composite Materials, 2012. **46**(6): p. 627-639.
45. Centea, T., L.K. Grunenfelder, and S.R. Nutt, *A review of out-of-autoclave prepregs – Material properties, process phenomena, and manufacturing considerations.* Composites Part A: Applied Science and Manufacturing, 2015. **70**: p. 132-154.

Figure Captions

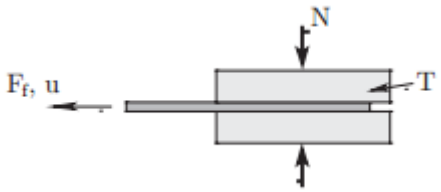

Figure 1: Schematic of the pull-out test method

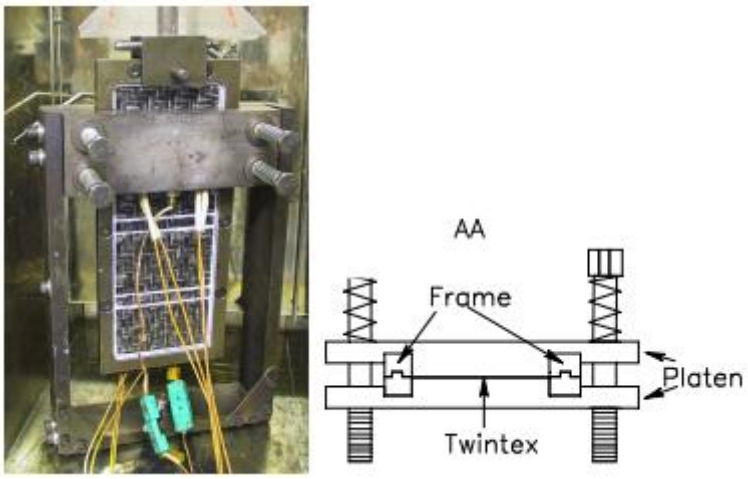

Figure 2: Left: photo of pull-through rig. Right: Schematic of top view of the rig

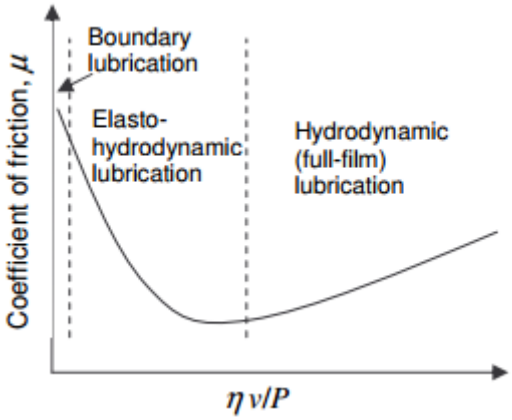

Figure 3: Typical Stribeck curve showing the different lubrication regimes

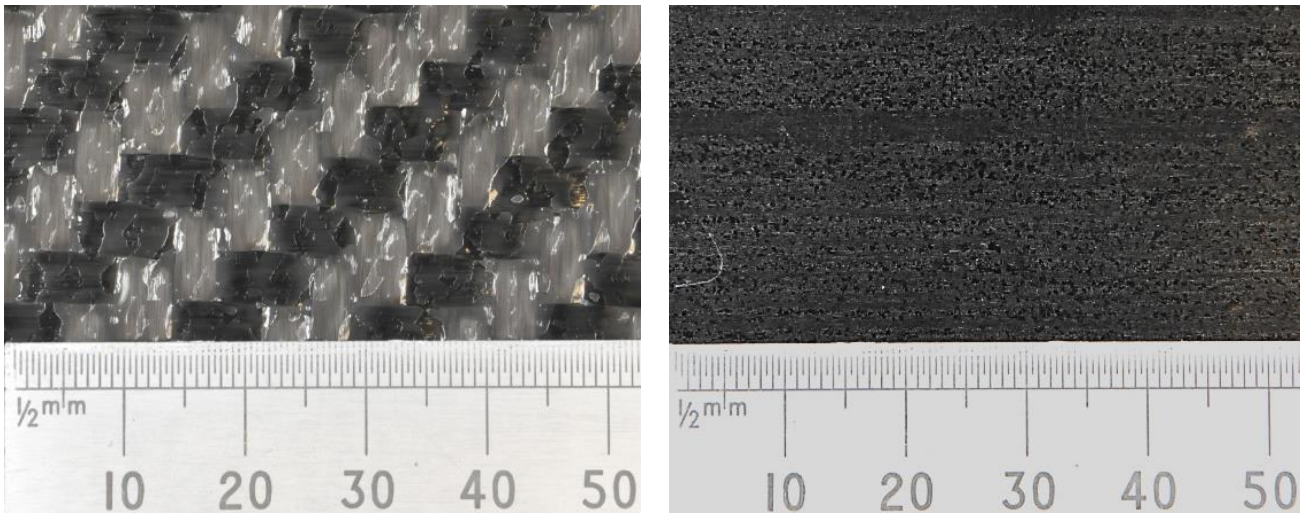

Figure 4: Materials tested; (left) 12k 2*2 Twill thermoset prepreg and (right) 15k unidirectional thermoset prepreg

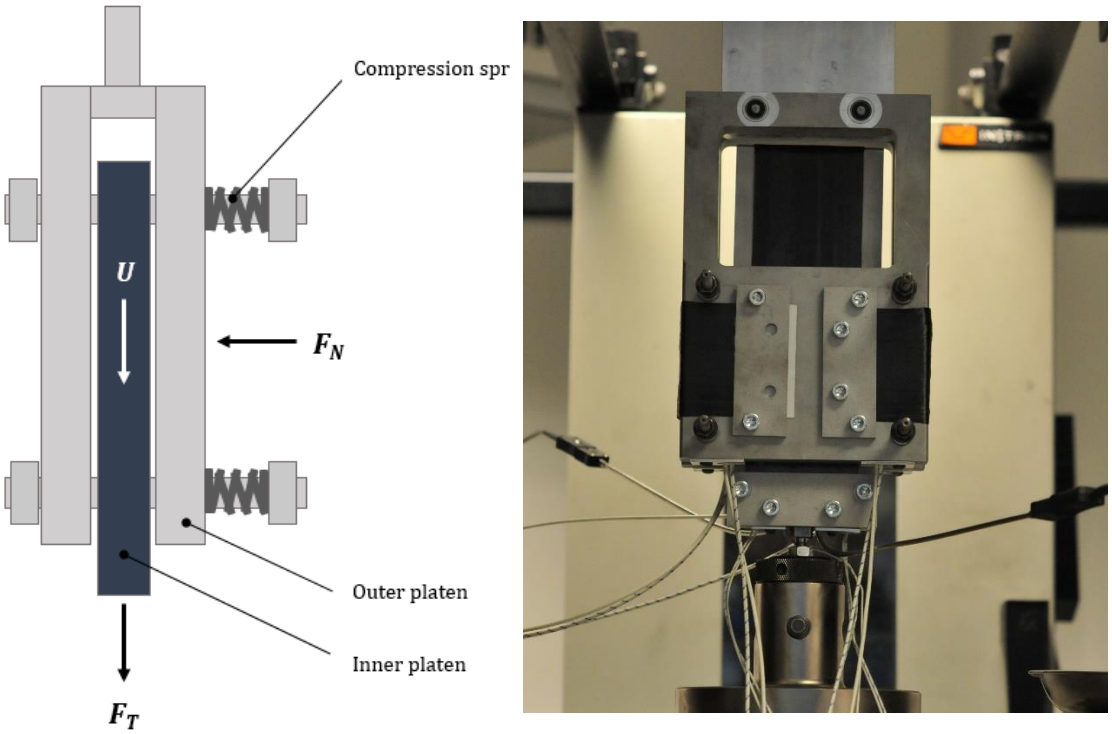

Figure 5: Interply friction rig. Left: schematic of the rig showing working principles. Right: Picture of the rig

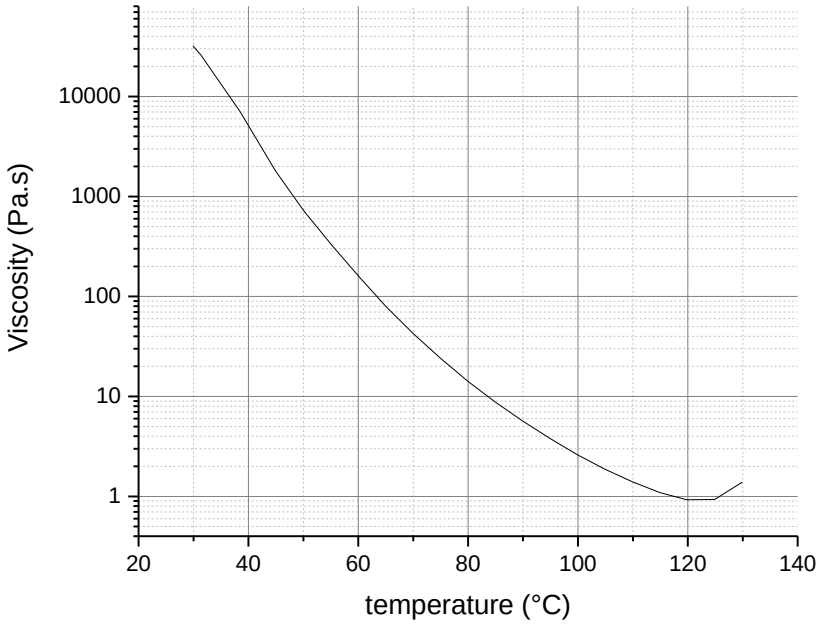

Figure 6: Viscosity-temperature curve for the resin used – Courtesy of Mitsubishi Chemical Carbon Fiber and Composites

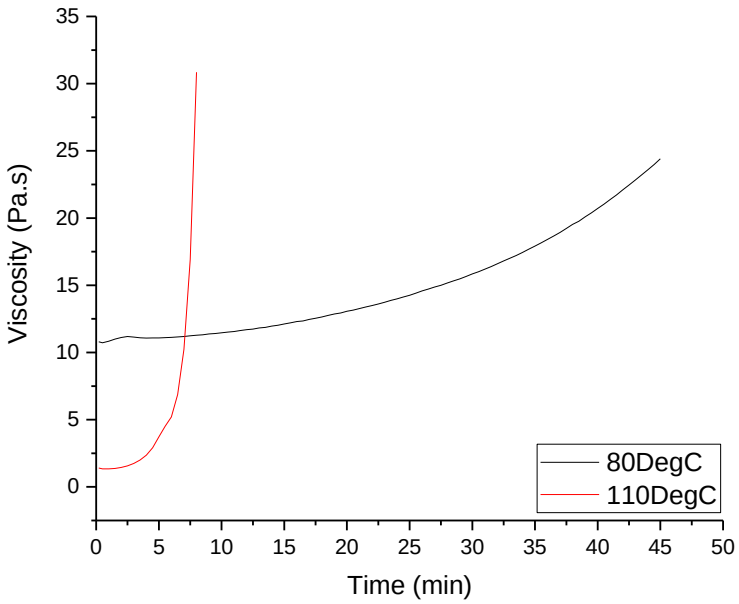

Figure 7: Isothermal viscosity profile at 80°C and 110°C - Courtesy of Mitsubishi Chemical Carbon Fiber and Composites

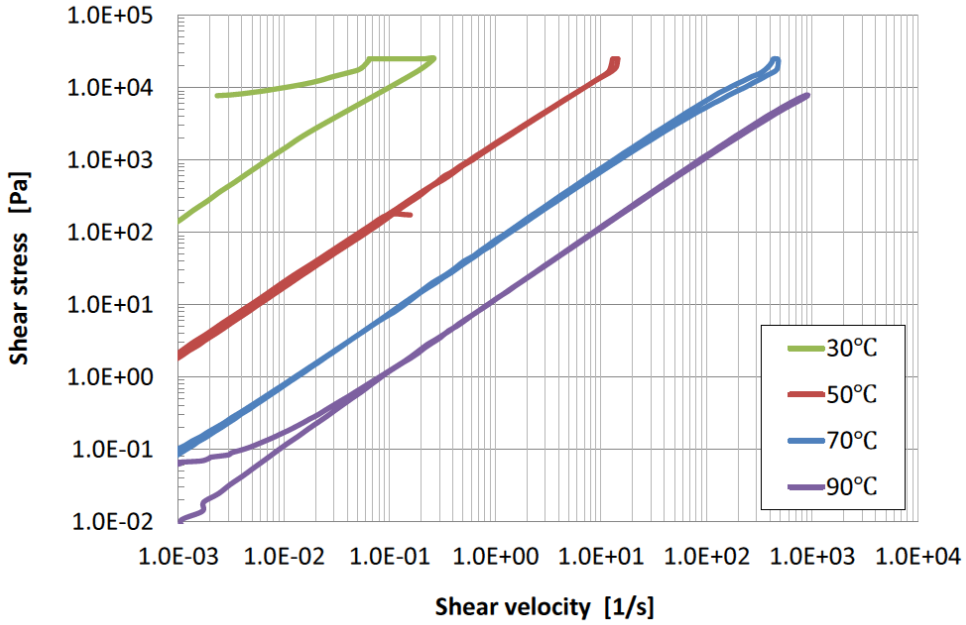

Figure 8: Shear stress as a function of shear rate for the resin used - Courtesy of Mitsubishi Chemical Carbon Fiber and Composites

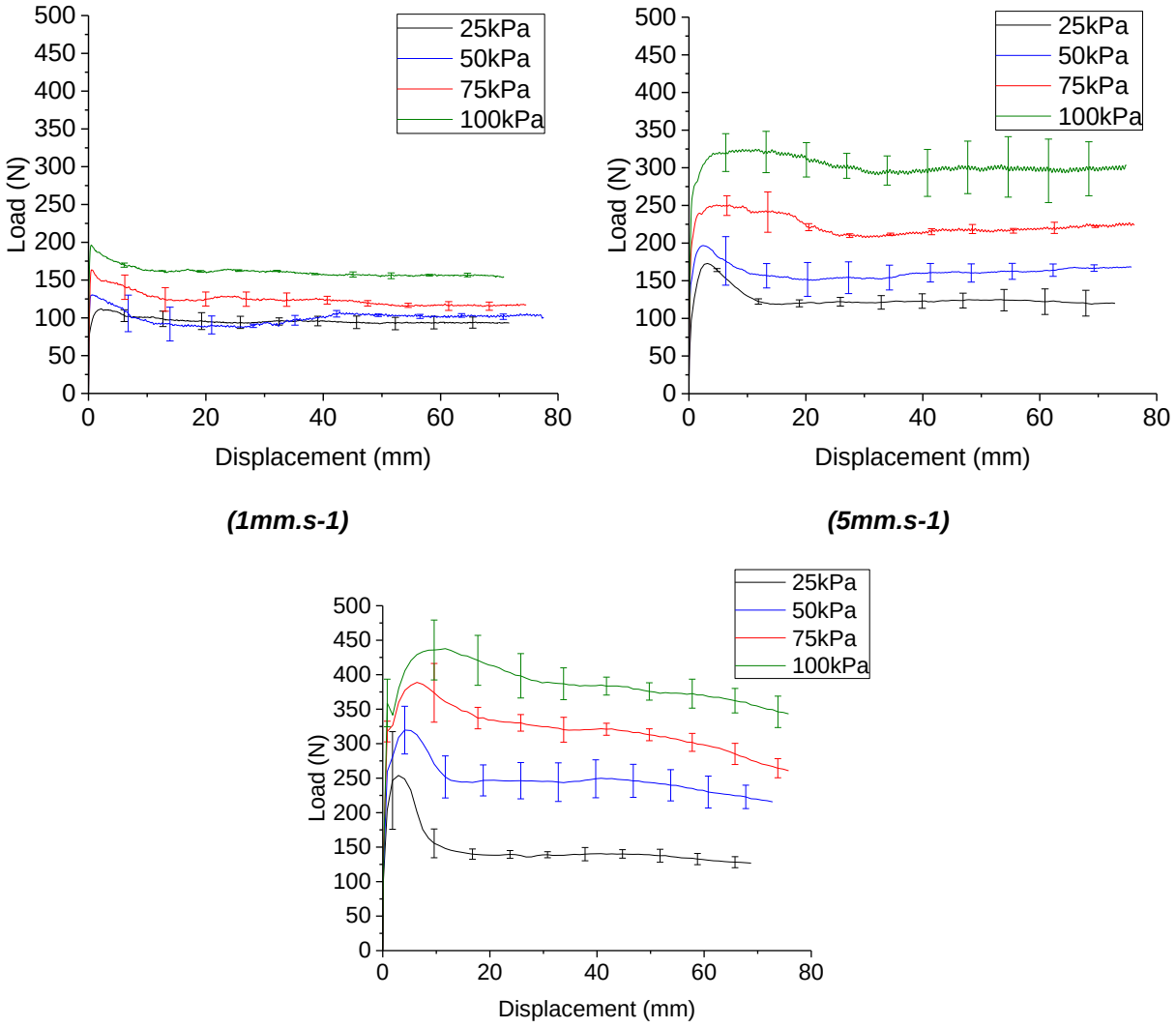

(1mm.s-1) ***(5mm.s-1)***

(10mm.s-1)

Figure 9: Influence of the normal pressure on the frictional load for the UD material tested at:

1mm.s-1, 5mm.s-1 and 10mm.s-1

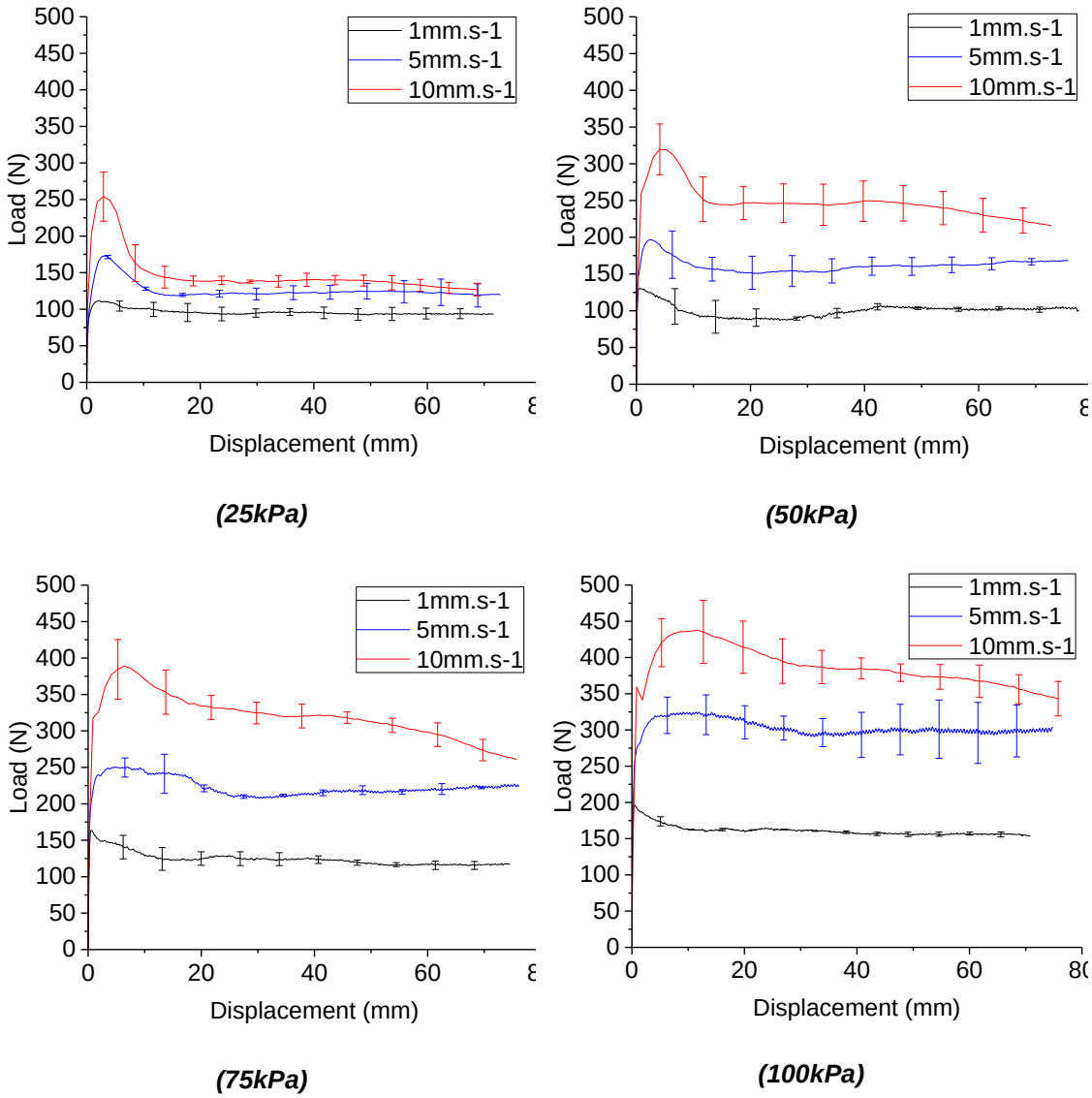

Figure 10: Influence of the sliding velocity on the frictional load for the UD material tested at 25kPa, 50kPa, 75kPa and 100kPa

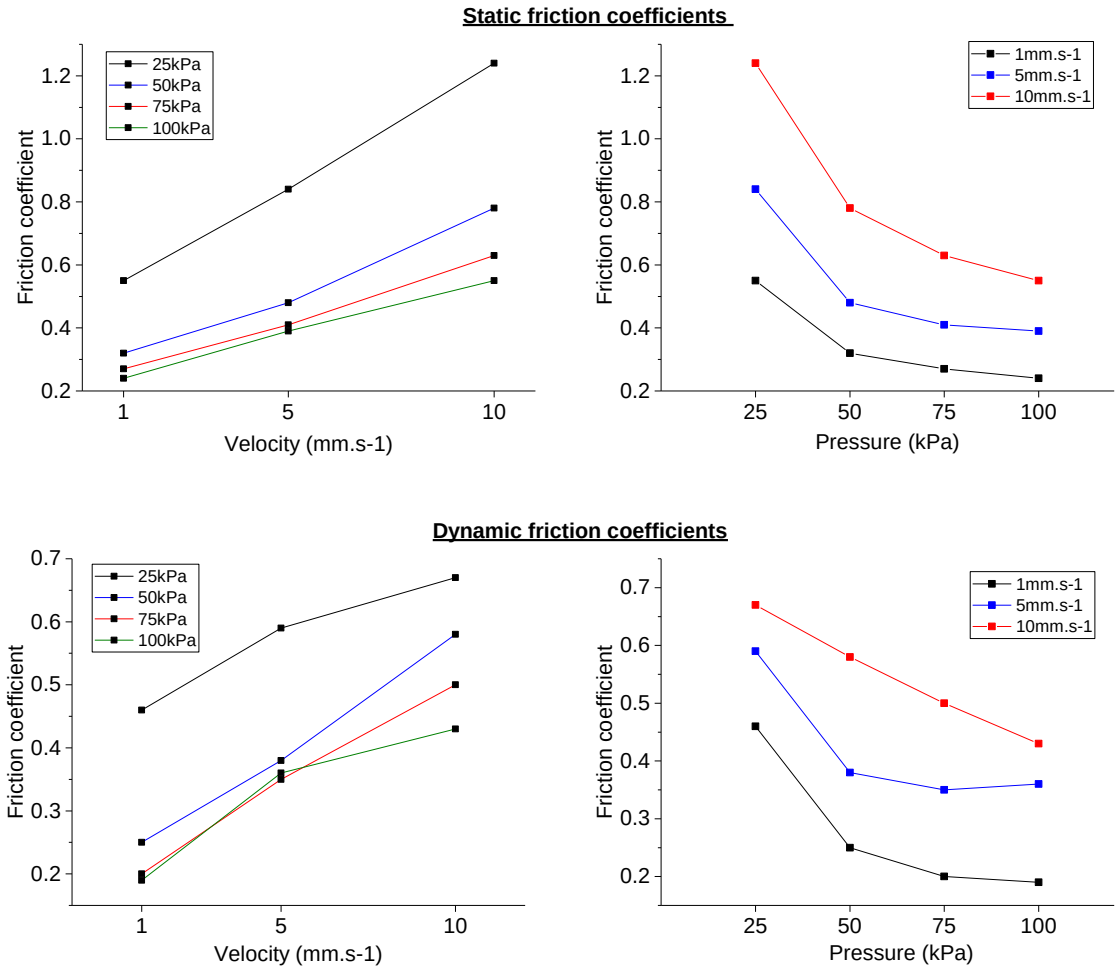

Figure 11: Evolution of the static (top) and dynamic (bottom) friction coefficients as a function of velocity (left) and normal pressure (right)

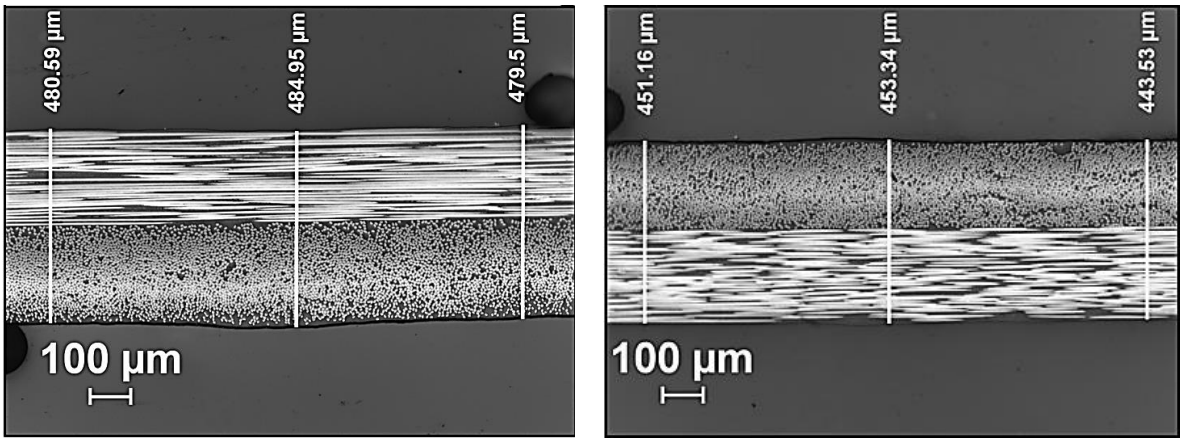

Figure 12: Cross-section micrographs showing the interface between two UD plies after a friction test performed with a normal pressure of 25kPa (left), and 100kPa (right) – (x10)

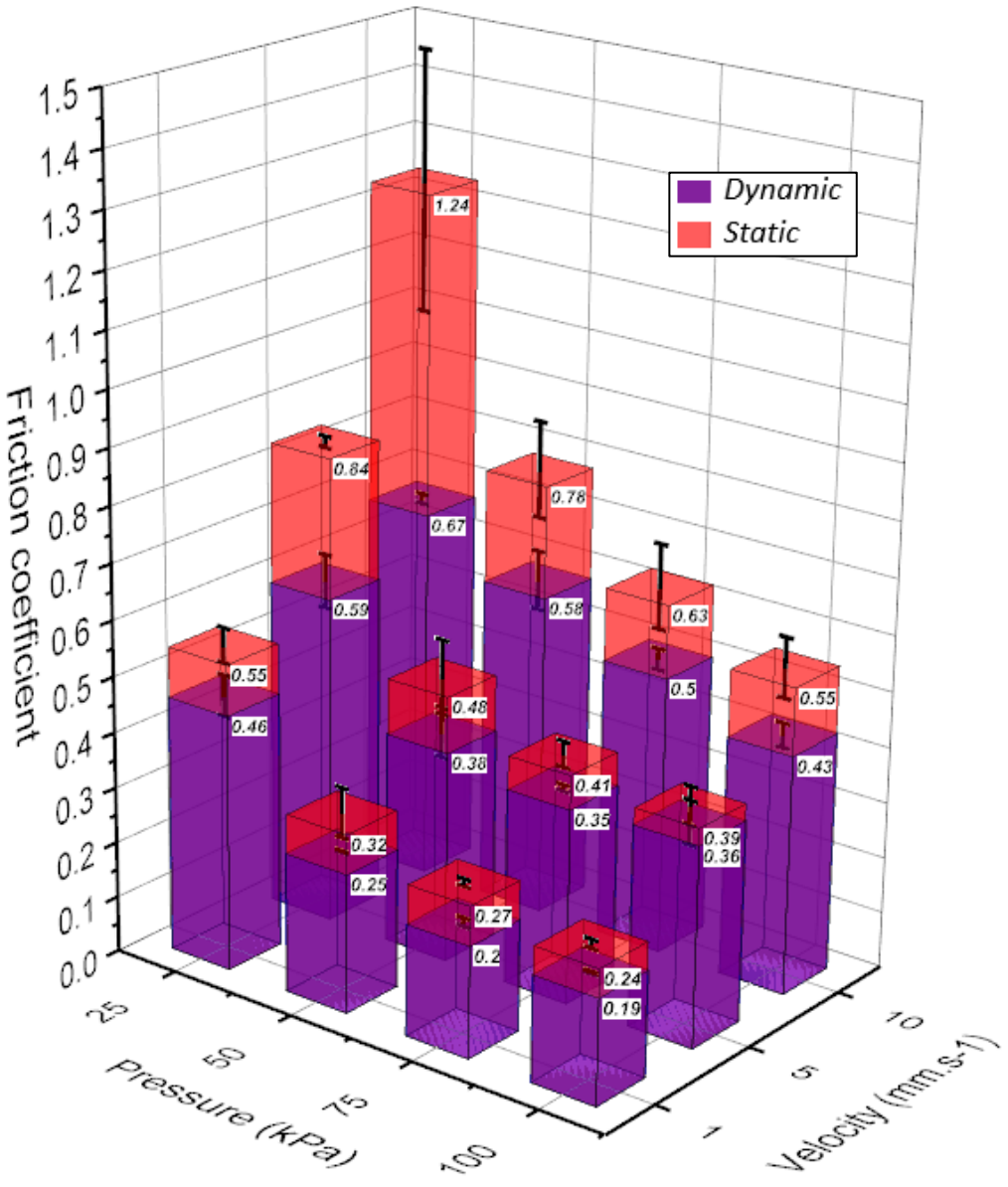

Figure 13: Friction coefficients summary for the UD material tested at different velocities and normal pressures.

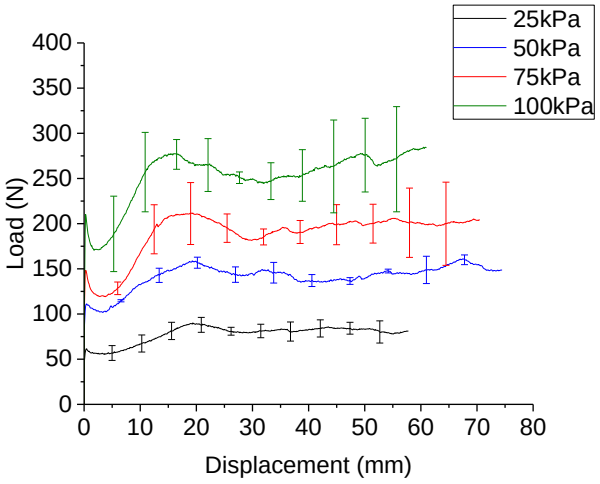

(1mm.s-1)

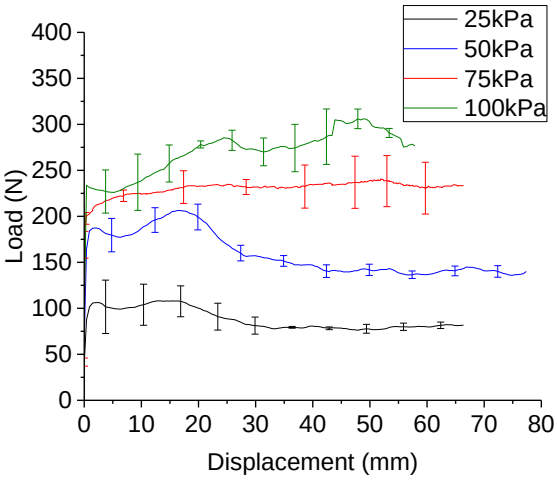

(5mm.s-1)

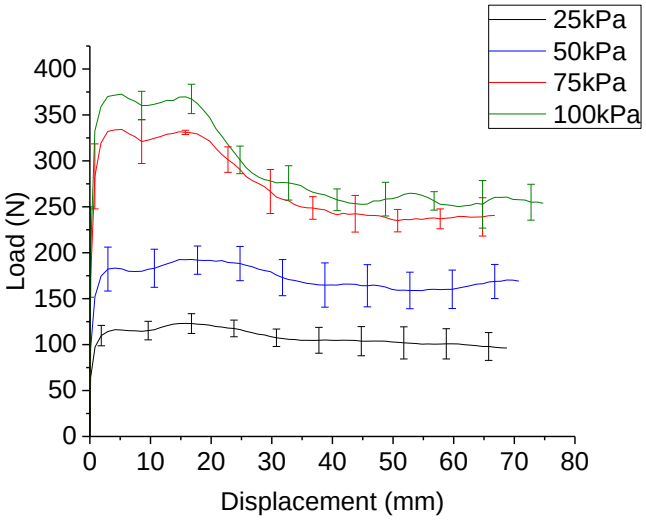

(10mm.s-1)

Figure 14: Influence of the normal pressure on the frictional load for the Woven material tested at: 1mm.s-1, 5mm.s-1 and 10mm.s-1

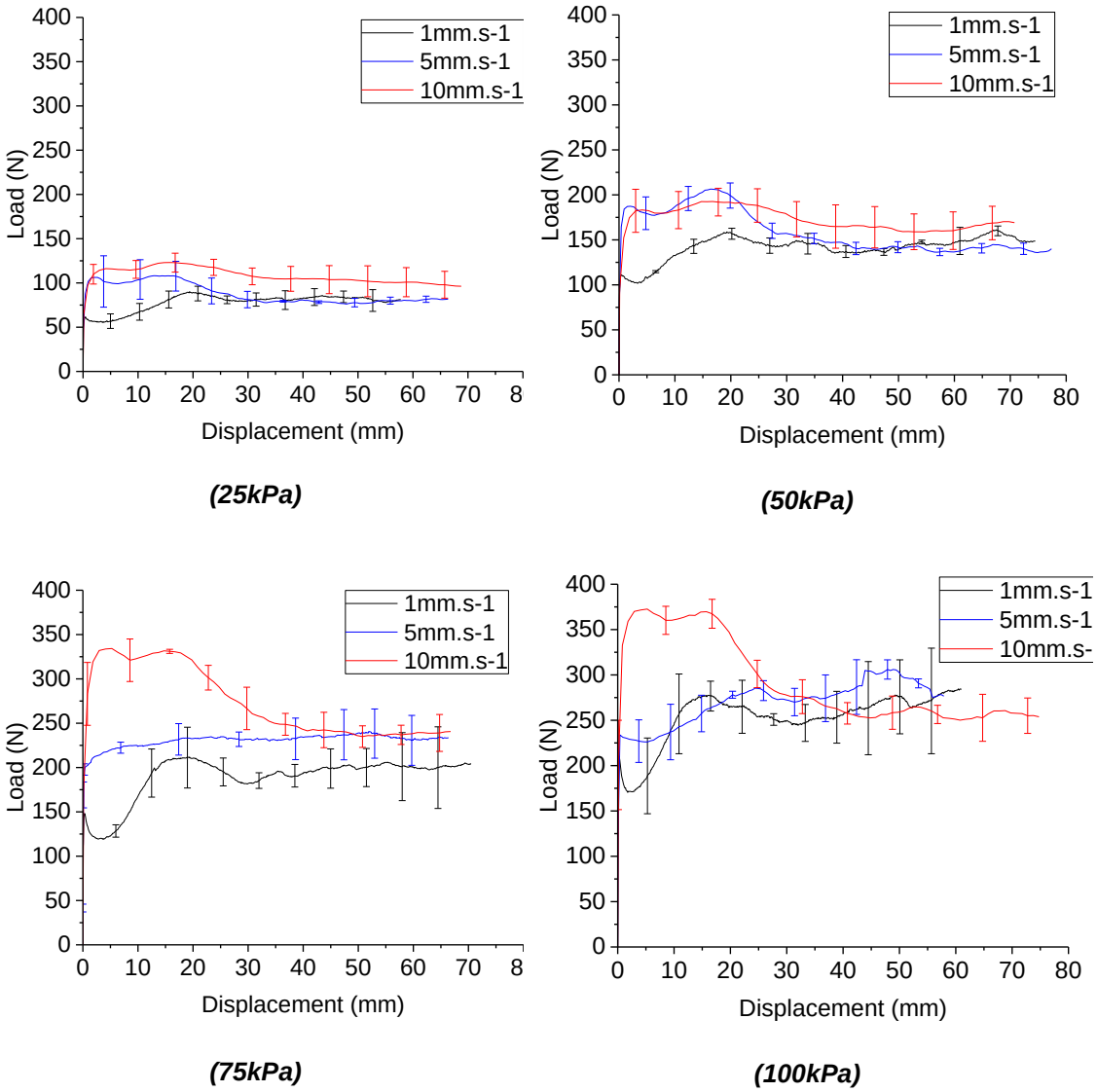

Figure 15: Influence of the sliding velocity on the frictional load for the Woven material tested at 25kPa, 50kPa, 75kPa and 100kPa

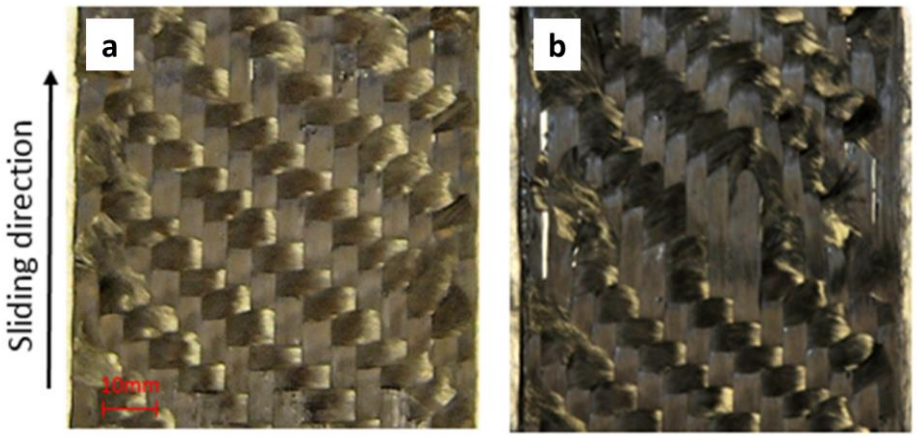

Figure 16: Pictures of a twill woven specimen after a friction test at 1mm.s-1 performed with a normal pressure of (a) 25kPa and (b) 100kPa.

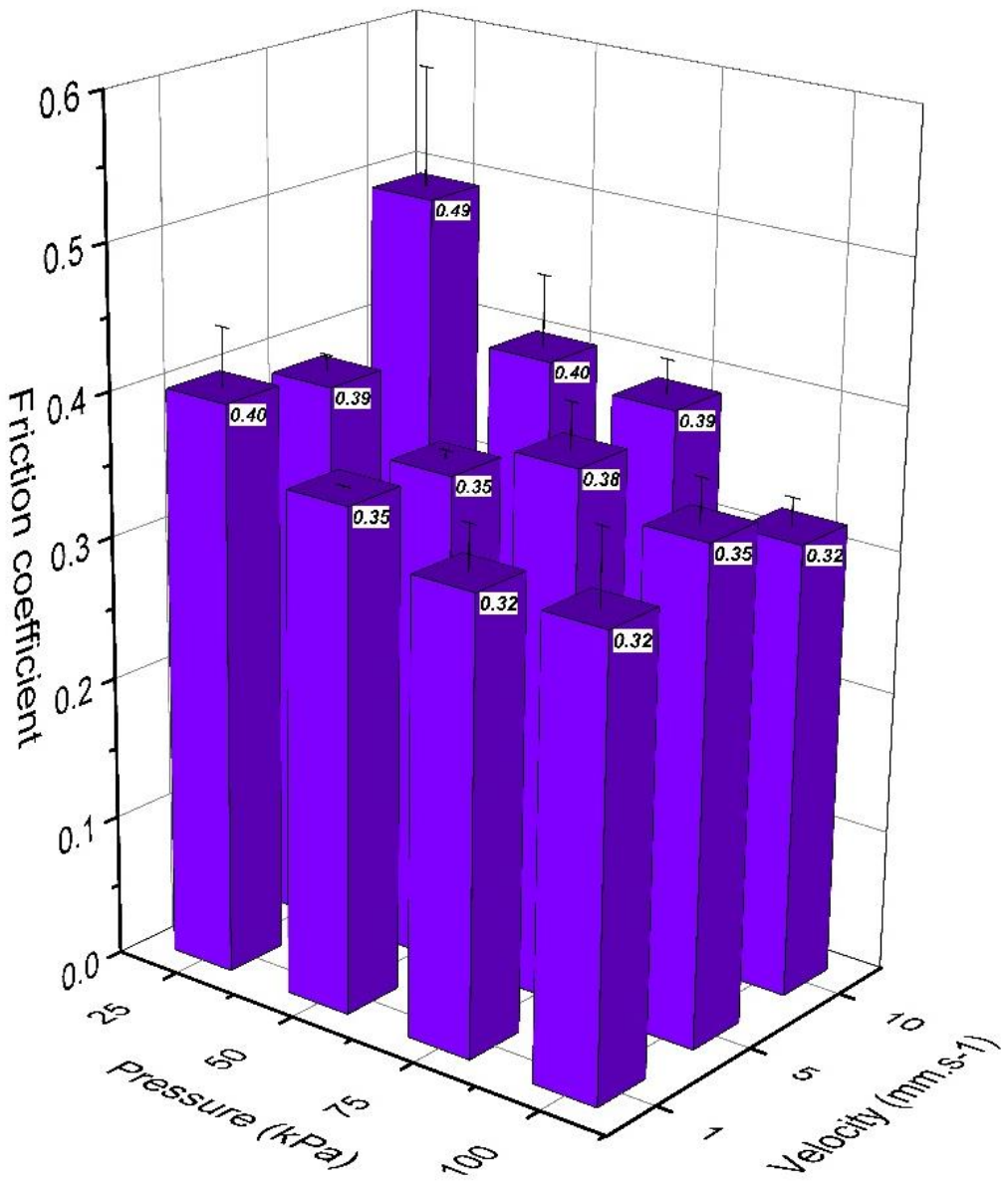

Figure 17: Dynamic friction coefficients summary for the Woven material at different test conditions.

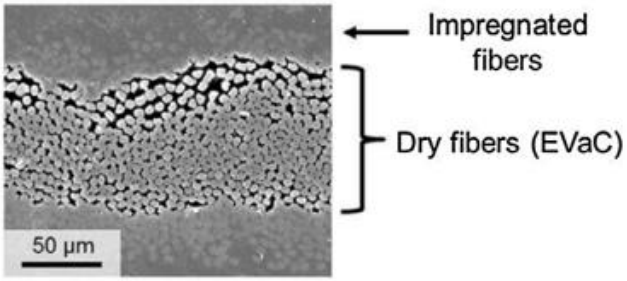

Figure 18: SEM micrograph of OOA prepreg showing air evacuation channels [45]

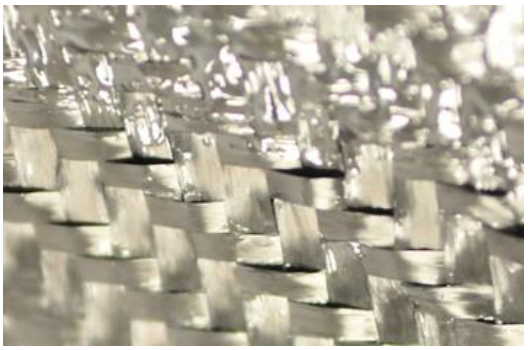

Figure 19: Picture showing the surface of a ply after a friction test performed with a normal pressure of 100kPa and the resin squeeze out effect.

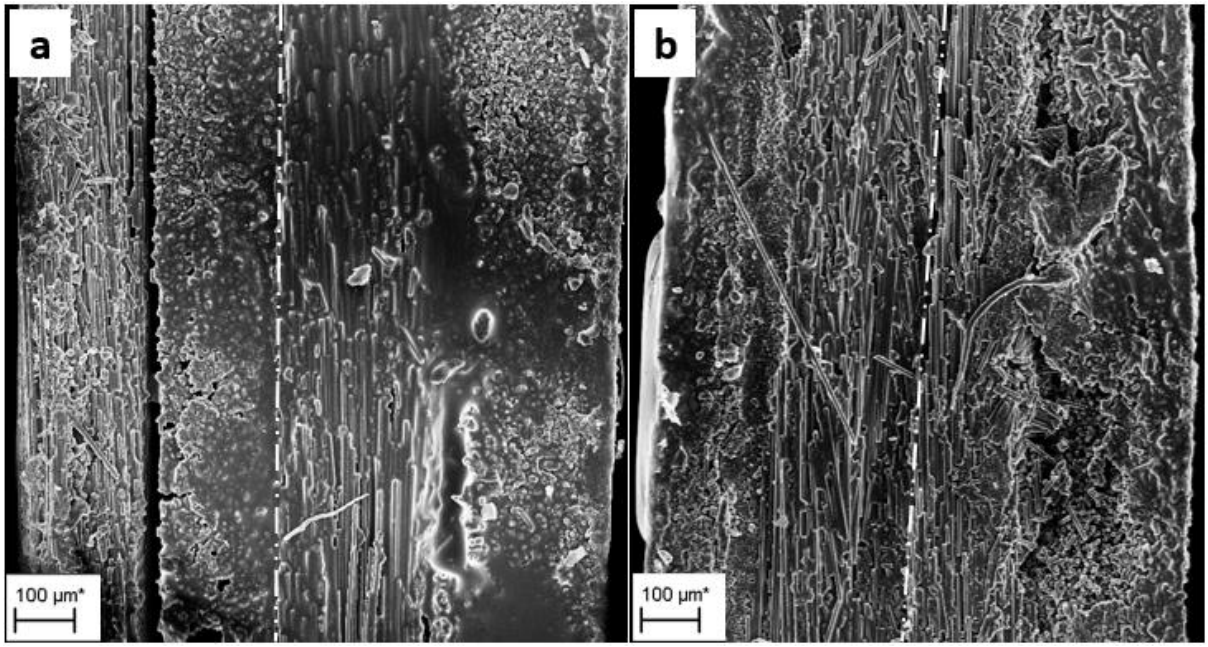

Figure 20: Cross-section SEM micrographs showing the interface between two plies of woven prepreg after a friction test performed with a normal pressure of (a) 25kPa and (b) 100kPa (x195). The white dotter lines represent the interface between the two woven plies.

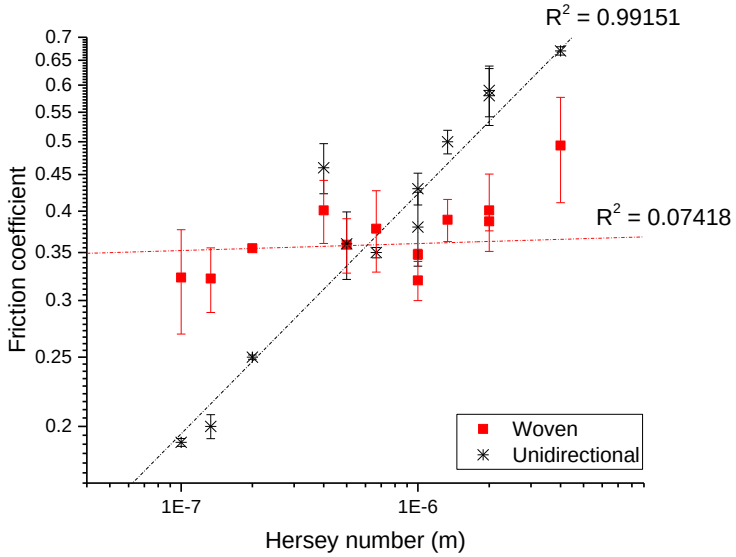

Figure 21: Stribeck curve for the woven and unidirectional material